

Evaluating the Performance of a Real-Time Electron Radiation Belt Specification Model

Frances Staples¹ · Adam Kellerman¹ · Janet Green²

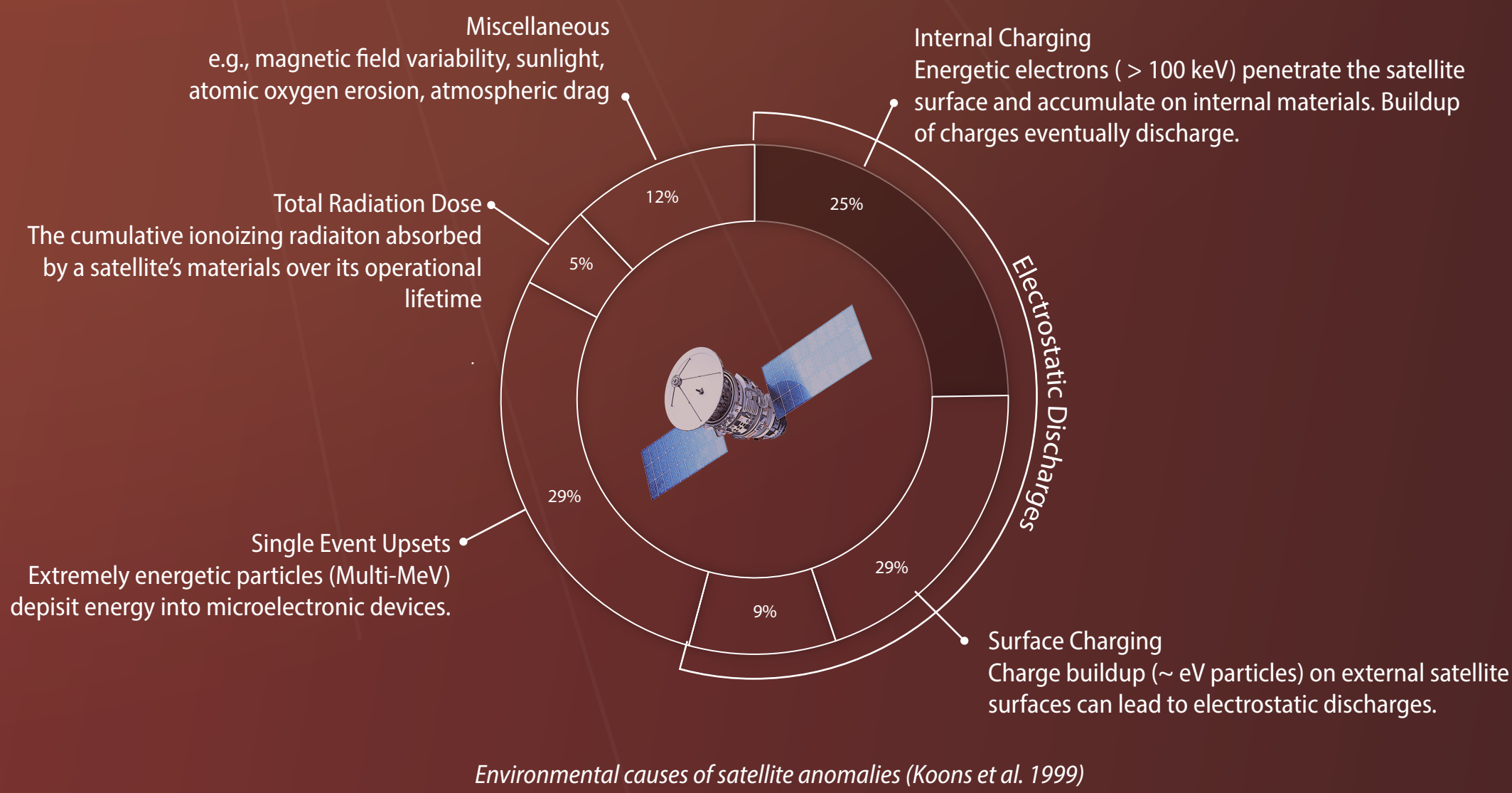
¹UCLA · ²Space Hazard Applications

Project Aims

- To evaluate the accuracy of the radiation environmental modelling used as input to the Satellite Charging Assessment Tool (SatCAT).
- Identify areas where the radiation belt model needs to be improved.

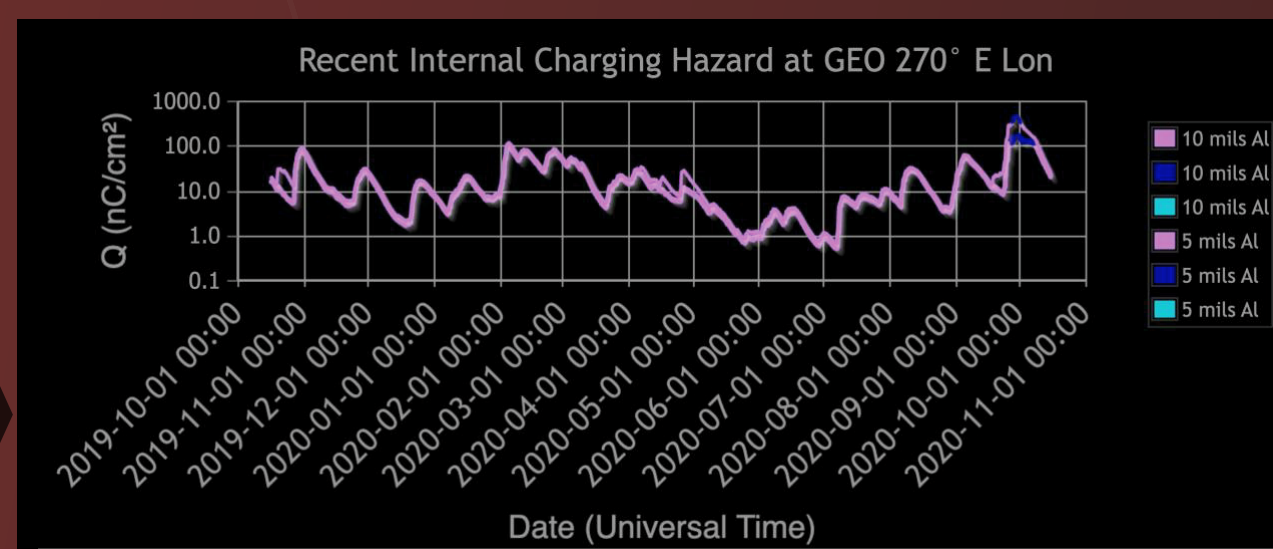
Motivation: Satellite Anomaly Attribution

Satellite anomalies are unexpected malfunctions or deviation in a satellite's operation, caused by factors such as hardware failure, software glitches, or environmental conditions like space weather. Anomalies range from minor malfunctions, to component damage or system failure.



Having the capability to attribute the cause of a satellite anomalies is crucial for implementing targeted corrective measures and enhancing future mission reliability. The Satellite Charging Assessment Tool (SatCAT) allows operators to monitor the real-time and longterm effects of internal spacecraft charging due to radiation belt electrons, which is a primary cause of satellite anomalies.

Radiation Environment Modelling (RBFMF)



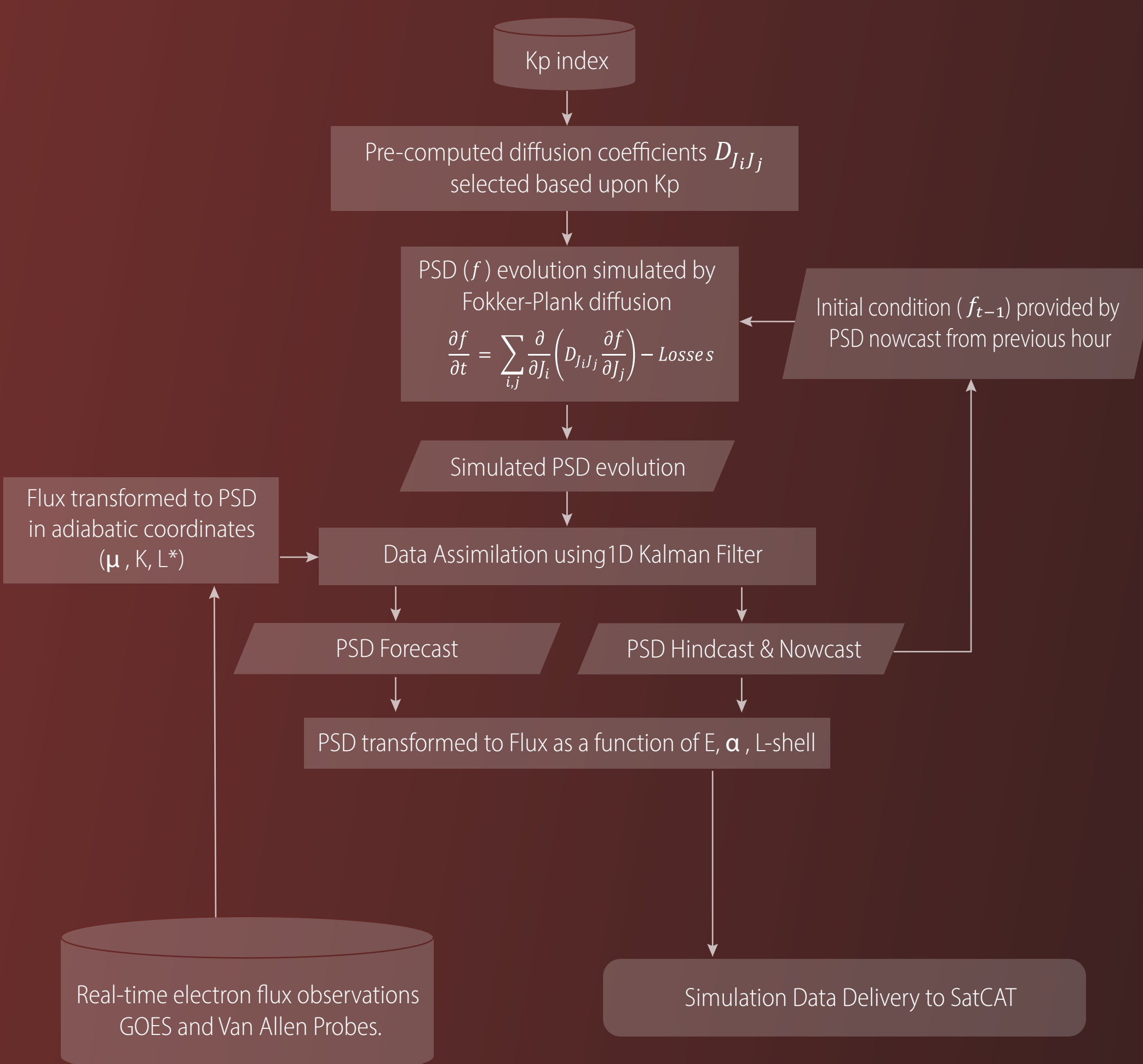
SatCAT display outputs: Charge accumulation, Q , is shown over time for user-defined orbits (GEO) and user-defined levels of component shielding. <http://spacehaz.com/satcat.html>

The Radiation Belt Forecasting Model and Framework

The Radiation Belt Forecasting Model and Framework (RBFMF) provides hourly hindcasts (previous 8 days) and forecast (future 2 days) of the electron radiation environment in real time (see Figure 1a).

RBFMF combines diffusive modelling of the radiation belt with real-time data inputs from GOES and Van Allen Probe beacon data (which was a pre-processed version of the final science ready data products).

Diffusion coefficients are modelled for wave-particle interactions with ULF (Brautingham & Albert 2000), Low-band chorus (Shprits et al., 2007; Li et al., 2007), and plasmaspheric hiss (Spasojevic et al., 2015) waves.



Contact: fastaples@atmos.ucla.edu

References:
 Agapitov et al. (2020) Geophys. Res. Lett., 47(13) DOI: 10.1029/2020GL088052;
 Bloch et al. (2021) Earth and Spc. Sci., 8(6) DOI: 10.1029/2020EA001610; Brautingham & Albert (2000) J. Geophys. Res., 105(A1) DOI: 10.1029/1999JA000344; Li et al. (2007) J. Geophys. Res., 112(A10) DOI: 10.1029/2007JA012368; Murphy et al. (2023) Space We., 45(9) DOI: 10.1002/2017GL076674; Ross et al. (2020) Geophys. Res. Lett., 47(20) DOI: 10.1029/2020GL088976; Shprits et al. (2007) J. Geophys. Res., 112(A12) DOI: 10.1029/2007JA012579; Spasojevic et al. (2015) J. Geophys. Res., 120(12) DOI: 10.1002/2015JA021803; Tsyganenko (1989) Plan. and Spc. Sci., 37(1) DOI: 10.1016/0032-0633(89)90066-4; Wong et al. (2024) J. Geophys. Res., 129(1) DOI: 10.1029/2023JA031607.

Read the Manuscript

View SatCAT

Validation Method

The 10-hour hindcast is validated against a dataset of PSD observations from 32 individual satellites from the Van Allen Probes, GOES, THEMIS, Cluster, MMS and GPS constellation.

Multi-Mission Observations:

Observations are converted to adiabatic coordinates using the IGRF and Tsyganenko (1989) field model, then intercalibrated at conjunctions in phase space with Van Allen Probe B and bias corrected GOES 15 data, which are chosen as "gold standard" PSD observations are interpolated across μ and K , and averaged across L^* and time to match the resolution of the simulation.

Statistical Evaluation:

The long term stistical error and bias is quantified using the median symmetric accuracy (MSA) and signed symmetric percentage bias (SSPB), described by Morley et al. (2018), where Q_i is the ratio between the hindcast and observation.

$$MSA = 100 (\exp (M(|\log_e(Q_i)|) - 1))$$

$$SSPB = 100 \operatorname{sgn}(M(\log(Q_i))) (\exp (M(|\log(Q_i)|) - 1))$$

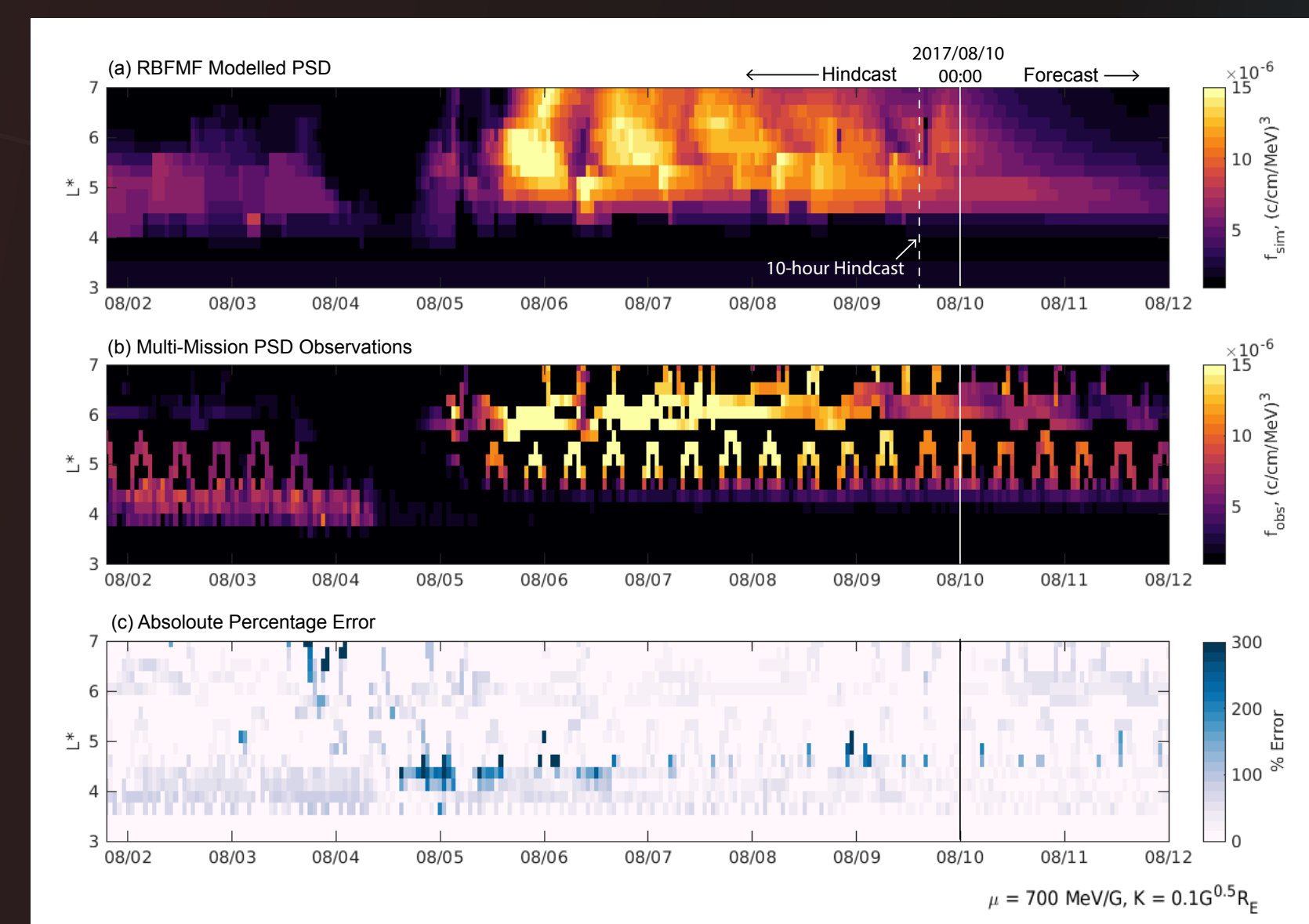
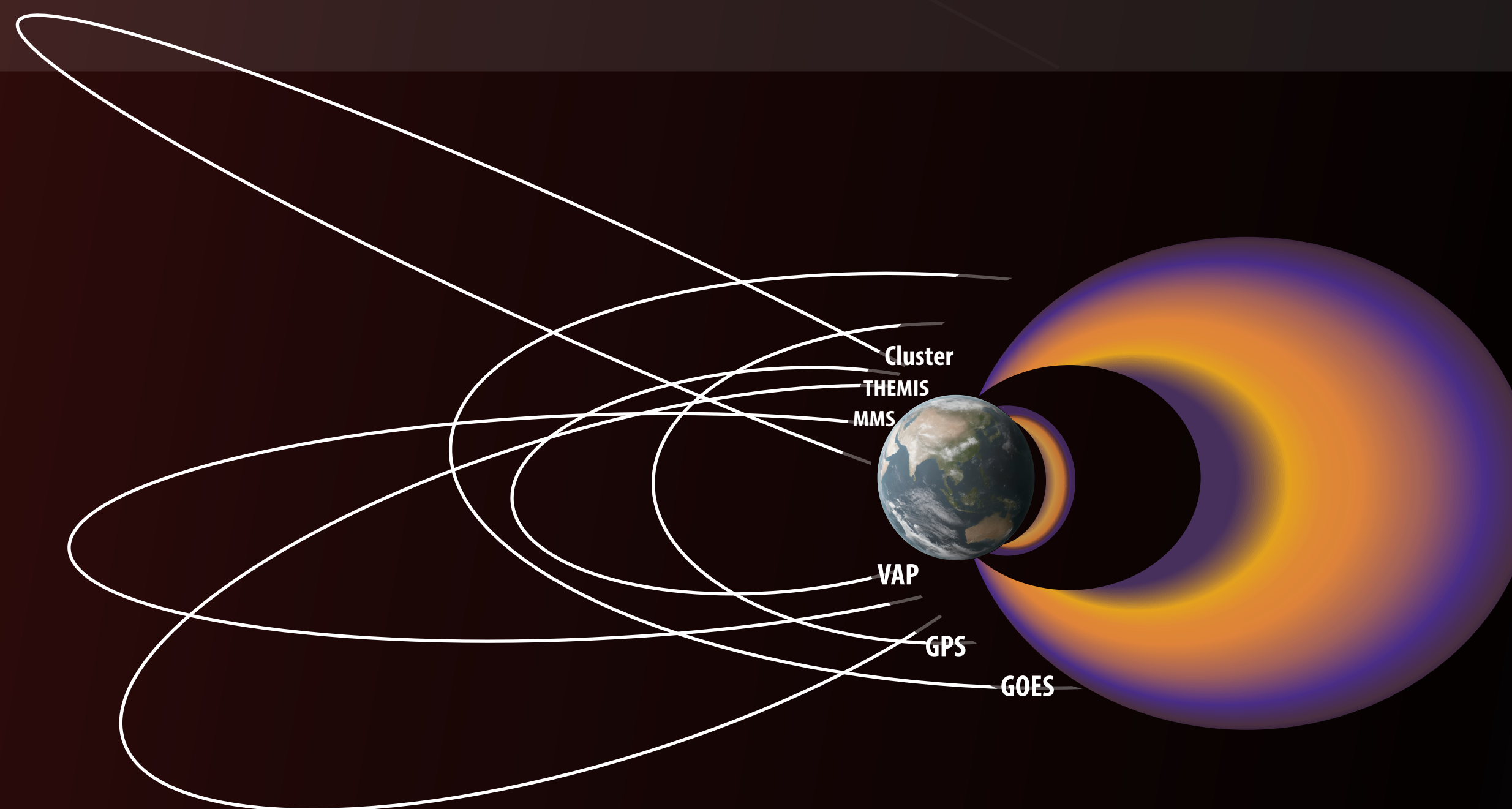


Figure 1. (a) Simulated radiation belt PSD at 00UT on 10th Aug 2017 as a function of L^* over time for $\mu = 700 \text{ MeV/G}$ and $K = 0.1 \text{ G}^{0.5} R_E$. (b) Corresponding PSD observations taken by multi-mission dataset. (c) Percentage error of RBFMF compared to observations $((f_{\text{hindcast}} - f_{\text{obs}}) / f_{\text{obs}}) \times 100$.



Analysis

Overall Performance (2016-2018)

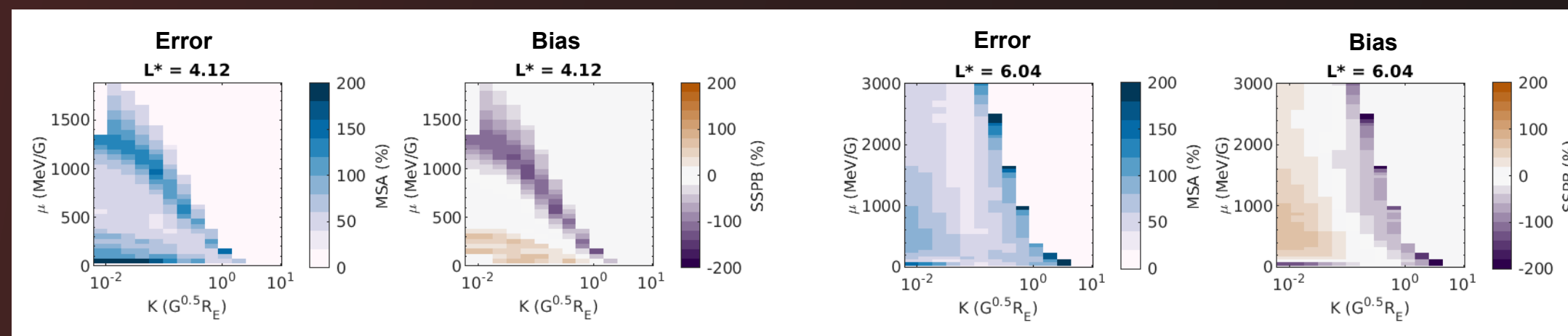


Figure 2: MSA (error) and SSPB (bias) between 2016-2019 are plotted for the 10-hour hindcast at $L^* = 4.12$ (left 2 panels) and $L^* = 6.04$ (right 2 panels), shown as function of μ and K .

Storm-time Assesment

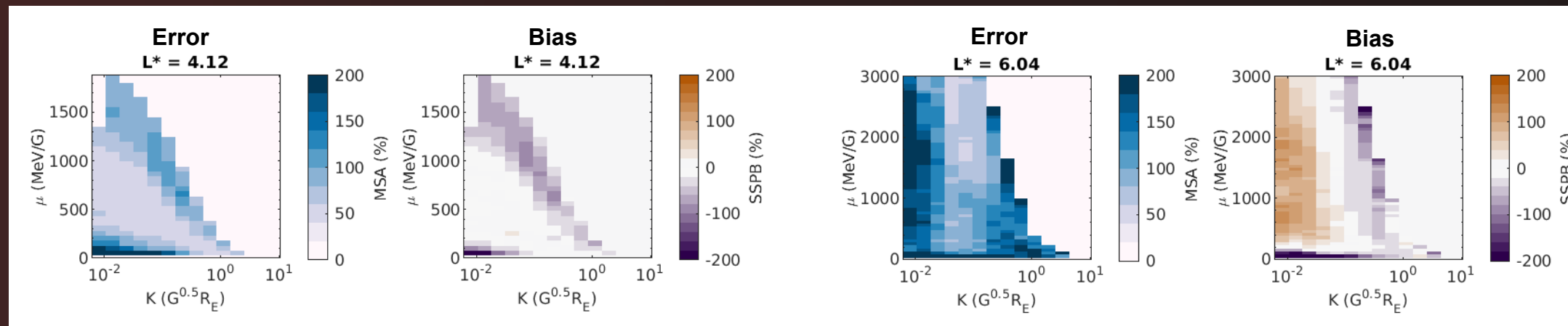


Figure 3: MSA (error) and SSPB (bias) of the 10-hour hindcast are calculated for geomagnetic storms occurring between 2016-2019. Storms are classified by Sym-H minima following a decrease from 15 nT to $< -40 \text{ nT}$.

Influence of Assimilated Data

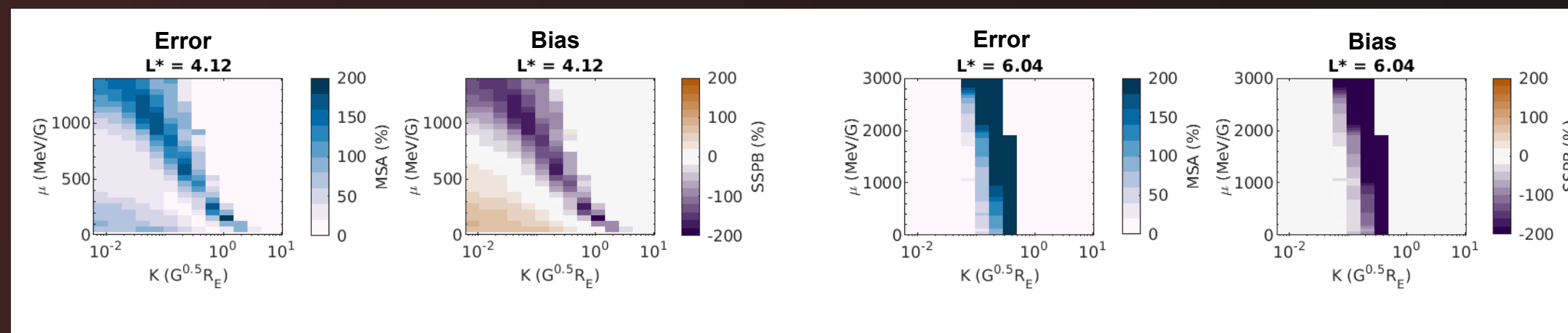


Figure 4: MSA (error) and SSPB (bias) of the Van Allen Probe-B beacon data when compared to the final Van Allen Probe-B science data product between 2016-2019.

Post Van Allen Probe Decomission (2019 - 2020)

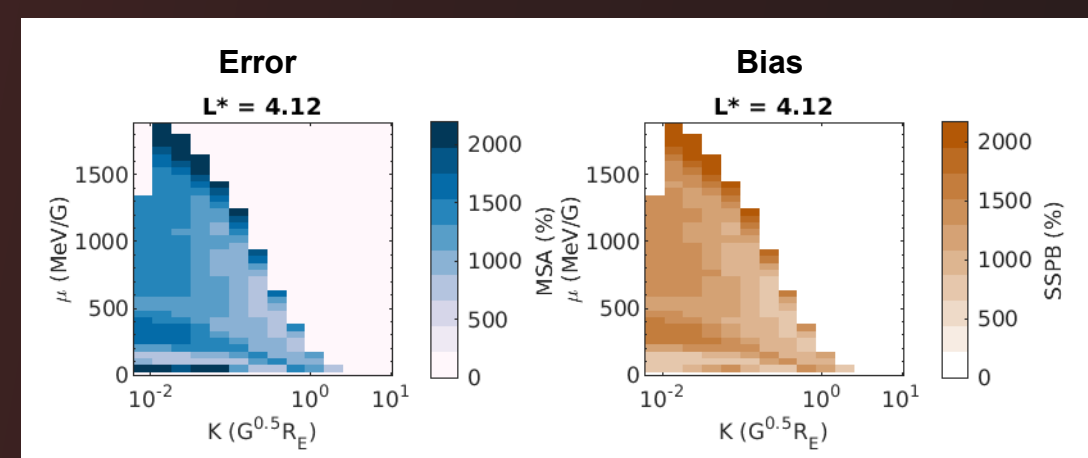


Figure 5: MSA (error) and SSPB (bias) of the 10-hour hindcast at $L^* = 4.12$ is plotted as function of μ and K for the years 2019-2020. MSA and SSPB are calculated by comparing the 10-hour hindcast to GPS data.

We do not validate $L^* = 6.04$ because real-time GOES data assimilated into the model is similarly processed to final GOES test data.

The outer radiation belt errors were < 150%.

Error and bias depended strongly upon μ , K , and L^* : PSD at high μ ($E > 700 \text{ keV}$) was biased toward underestimation by up to 150%, and PSD at low μ ($E < 300 \text{ keV}$) was biased toward overestimation by up to 70%.

PSD at $\mu < 500 \text{ MeV/G}$ ($E < 700 \text{ keV}$) was underestimation at greater rates during storm times. This was associated with substorm injections which were not included in the model.

PSD of equatorial electrons ($K < 0.1 \text{ G}^{0.5} R_E$) was overestimated at $L^* = 6.04$, suggesting outer loss processes were not well captured by the model.

Van Allen Probe data greatly influenced hindcast bias, shown by matching relationships in bias when beacon data was tested against final science data.

Prediction accuracy decreased by an order of magnitude at $L^* = 4.12$ when real time Van Allen Probe data were not available. This highlights the importance of observations through the whole radiation belt in this data assimilative model.

It is assumed that the hindcast retains high performance at $L^* = 6.04$ since GOES data continues to be assimilated.

Conclusion

Data assimilation substantially improved the error and bias of radiation belt specification but strongly influenced hindcast error and bias.

The RBFMF hindcast was accurate to within a factor of 1.5 in the outer radiation belt between 2016-2018

The highly simplistic physics based modelling must be improved now that real-time Van Allen Probe observations are no longer available.

New missions providing observations in the core of the radiation belt in real time are required to enable accurate forecasting of the radiation environment.

Future Model Development

Test new models of diffusion coefficients representing Hiss, Chorus, and ULF waves (e.g., Agapitov et al., 2020, Wong et al., 2024, Murphy et al., 2023).

Improve representation of storm time losses: EMIC wave scattering through new diffusion coefficients (e.g., Ross et al., 2020) and improving the dynamic outer simulation boundary (e.g., Bloch et al., 2021).

Simulate substorm injections through updates to the inner simulation boundaries.